From (20), we can see that $\mathbf{x}$ is correctly recovered if $Q_z\left[\frac{1}{2}\frac{\mathbf{n}}{\beta}\right]=\mathbf{0}$. This means that for a given noise power, the component $1/\beta$ will be the factor that determines the system performance. In Fig. 2 and Fig. 3, the empirical cumulative distribution functions (ECDFs) of the $1/\beta$ in (20) are shown for the LC-RBD-LR-ZF and LR-LGP precoders when the system is with and without transmit antenna selection. For the same system configuration, the simulation results show that the LC-RBD-LR-ZF precoder generates smaller $1/\beta$ than the LR-LGP precoder. This means that the LC-RBD-LR-ZF precoder will probably outperform the LR-LGP precoder for the same system configuration. Moreover, the more sub-groups are generated the smaller $1/\beta$ becomes, and hence the better system performance can be achieved. It can also be observed from the two figures that the transmit antenna selection technique allows the system to reduce $1/\beta$, thereby improving the system performance.

4.2. Computational Complexity Analysis

In this sub section, we evaluate the computational complexity of the proposed LR-LGP algorithm and the LC-RBD-LR-ZF algorithm in [12]. The complexities are evaluated by counting the required floating point operations (flops). We assume that each real operation (an addition, a multiplication or a division) is counted as a flop. Hence, a complex multiplication and a division equal to 6 flops and 11 flops, respectively. It is worth noting that the QR decomposition of an $r\times t$ complex matrix requires $6rt^2+4rt-t^2-t$ flops. Based on the above assumptions, the computational complexities of the proposed LR-LGP algorithm and the LC-RBD-LR-ZF one are computed in details as follows

a. Complexity of the LC-RBD-LR-ZF algorithm

The computational complexity of the LC-RBD-LR-ZF algorithm is given by:

$$F = F_a + F_b + F_c \ \ (flops). \tag{21}$$

herein F_a and F_b are the number of flops to calculate $\mathbf{P}_a$ and $\tilde{\mathbf{P}}_b$, respectively. F_c is the number of flops of the multiplication two matrices $\mathbf{P}_a$ and $\tilde{\mathbf{P}}_b$. F_a and F_b are evaluated and expressed in the (22) and (23).

$$\begin{aligned} F_a = K\big[&6(N_R-N_u)(N_R+N_T-N_u)^2 \\ &+4(N_R-N_u)(N_R+N_T-N_u)-(N_R+N_T-N_u)^2 \\ &-(N_R+N_T-N_u)\big] \qquad (flops) \end{aligned} \tag{22}$$

$$\begin{aligned} F_b = {}& K(8N_T^2N_u-2N_TN_u)+K(16N_u^2N_T-2N_uN_T \\ &+8N_u^3-2N_u^2+F_{update-LLL})+K(8N_u^3+16N_u^2N_T \\ &-2N_u^2-2N_uN_T) \quad (flops) \end{aligned} \tag{23}$$

Note that in (23), $F_{update-LLL}$ is the computational cost of the update operation for the LLL technique, which is obtained by computer simulation.

F_c is evaluated to be

$$F_c = 8KN_T^2N_R - 2N_TN_R \ \ (flops). \tag{24}$$

From (21)-(24), the total number of flops of the LC-RBD-LR-ZF algorithm is obtained as in (25).

$$\begin{aligned} F = {}& K\big[6(N_R-N_u)(N_R+N_T-N_u)^2 \\ &+4(N_R-N_u)(N_R+N_T-N_u)-(N_R+N_T-N_u)^2 \\ &-(N_R+N_T-N_u)\big]+K(8N_T^2N_u-2N_TN_u) \\ &+K(16N_u^2N_T-2N_uN_T+8N_u^3-2N_u^2+F_{update-LLL}) \\ &+K(8N_u^3+16N_u^2N_T-2N_u^2-2N_uN_T) \\ &+8KN_T^2N_R-2N_TN_R \quad (flops) \\ &\sim O(N_R^4) \end{aligned} \tag{25}$$

b. Complexity of the LR-LGP algorithm

The computational complexity of the proposed LR-LGP algorithm is given by

$$F_1 = F_A + F_B + F_C \ \ (flops). \tag{26}$$

where F_A and F_B are the number of flops to calculate $\mathbf{W}_a$ and $\mathbf{W}_b$, respectively. F_C is the number of flops of multiplying the two matrices $\mathbf{W}_a$ and $\mathbf{W}_b$.

F_A is expressed as

$$F_A = F_{MMSE} + F_{QR} \ \ (flops), \tag{27}$$

where F_{MMSE} is the number of flops to compute the $\mathbf{W}_{MMSE}$ matrix and F_{QR} is number of flops for the QR

decomposition operations. F_{MMSE} and F_{QR} are calculated as follows

$$F_{MMSE} = 8N_R^3 + 16N_R^2N_T - N_R^2 - 2N_RN_T + N_R + 1 \quad (flops). \tag{28}$$

$$F_{QR} = L(6N_T^2\alpha + 4N_T\alpha - \alpha^2 - \alpha) \ (flops). \tag{29}$$

Therefore, the total number of flops to find $\mathbf{W}_a$ is given by

$$\begin{aligned} F_A &= F_{MMSE} + F_{QR} \\ &= 8N_R^3 + 16N_R^2N_T - N_R^2 - 2N_RN_T + N_R \\ &+ 1 + L(6N_T^2\alpha + 4N_T\alpha - \alpha^2 - \alpha) \ (flops). \end{aligned} \tag{30}$$

F_B is calculated as follows

$$F_B = F_2 + F_3 + F_4 \quad (flops), \tag{31}$$

where F_2, F_3 and F_4 are the total number of flops to compute $\bar{\mathbf{H}}_l$, $\hat{\mathbf{H}}_l$ and $\mathbf{W}_b^{GP_l}$ matrices, respectively. F_2 and F_3 are computed as

$$F_2 = L(8N_T\alpha^2 - 2\alpha^2) \ (flops). \tag{32}$$

$$F_3 = F_5 + F_6 + F_{update-SLV} \quad (flops). \tag{33}$$

herein F_5 and F_6 are the number of flops to compute $\tilde{\mathbf{C}} = \left[\left\{\left(\bar{\mathbf{H}}_l^{ext}\right)^T\right\}^H \left(\bar{\mathbf{H}}_l^{ext}\right)^T\right]^{-1}$ and $\hat{\mathbf{H}}_l = \mathbf{U}_l^T\bar{\mathbf{H}}_l^{ext}$, respectively. $F_{update-SLV}$ is computational cost of the ELR-SLV algorithm's update operations, which is obtained by computer simulation. Therefore, F_3 is calculated as

$$F_3 = L(24\alpha^3 - 2\alpha^2) + L(16\alpha^3 - 4\alpha^2) + LF_{update-SLV} \quad (flops). \tag{34}$$

The number of flops to find all $\mathbf{W}_b^{GP_l}$ matrices is given by

$$F_4 = L(56\alpha^3 - 8\alpha^2) \quad (flops). \tag{35}$$

Hence, the total number of flops to find the precoding matrix $\mathbf{W}_b$ is represented by

$$F_B = L(8N_T\alpha^2 - 2\alpha^2) + L(24\alpha^3 - 2\alpha^2) + L(16\alpha^3 - 4\alpha^2) + LF_{update-SLV} + L(56\alpha^3 - 8\alpha^2)(flops). \tag{36}$$

F_C is calculated by

$$F_C = 8N_R^2N_T - 2N_R^2 \quad (flops). \tag{37}$$

From the above analysis results, the total number of flops for the LR-LGP algorithm is given in the (38)

$$\begin{aligned} F_1 &= 8N_R^3 + 16N_R^2N_T - N_R^2 - 2N_RN_T + N_R + 1 \\ &+ L(6N_T^2\alpha + 4N_T\alpha - \alpha^2 - \alpha) + L(8N_T\alpha^2 - 2\alpha^2) \\ &+ L(24\alpha^3 - 2\alpha^2) + L(16\alpha^3 - 4\alpha^2) + LF_{update-SLV} \\ &+ L(56\alpha^3 - 8\alpha^2) + 8N_R^2N_T - 2N_R^2 \ (flops). \\ &\sim O(N_R^3) \end{aligned} \tag{38}$$

5. Simulation results

In this section, we evaluate and compare not only the BER performance but also the computational complexity of the LR-LGP precoder with those of the LC-RBD-LR-ZF precoder in [12]. The channel between the BS and all users are assumed to be semi-static Rayleigh fading.

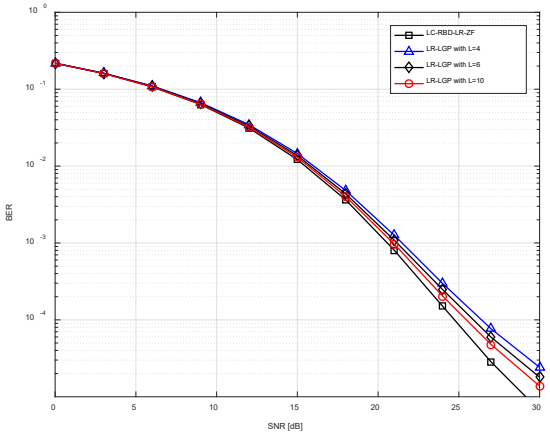

Figure 4. The system performance with $N_T = M = 60$, $N_u = 1, K = 60, L = 4, 6, 10.$

Fig. 4 illustrates the system performance for the proposed algorithm LR-LGP and the LC-RBD-LR-ZF algorithm in [12]. The simulation parameters are as follows: $N_T = M = 60$, $N_u = 1$, $K = 60$ and 4-QAM modulation. The number of user groups for the LR-LGP precoder is L = 4; 6, and 10. The simulation results in Fig. 4 show that the BER performance of the proposed algorithm LR-LGP is asymptotic to the LC-RBD-LR-ZF algorithm when L increases. Specifically, at $BER = 10^{-3}$ the proposed algorithm suffers from performance degradations of around 0.5 dB, 0.8 dB and 1.1 dB in SNR corresponding to L = 10; 6 and 4 when compared to the LC-RBD-LR-ZF algorithm. However, the computational complexity of the proposed algorithm

is significantly lower than the LC-RBD-LR-ZF algorithm, as confirmed by the simulation results in Fig. 7.

Fig. 5 and Fig. 6 illustrate the system performance when the TA-GS technique is applied. To get the results, the following parameters are used: $M = 90$, $N_T = 60$, $N_u = 1, K = 60, L = 4,6,10$, 4-QAM modulation, $\delta = 2$ for Fig. 5 and $\delta = 3$ for Fig. 6. It can be seen from the figures that the system performance is significantly improved as the TA-GS technique is adopted. Specifically, at $\text{BER} = 10^{-3}$ for the same precoder, the system performance improves by about 2 dB and 1.5 dB in SNR corresponding to $\delta = 2$ and $\delta = 3$ when compared to the case of no antenna selection. Besides, Fig. 5 and Fig. 6 show that the performance improvement is inversely proportional to δ.

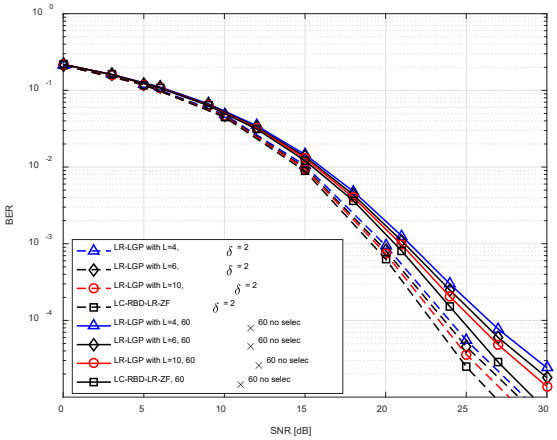

Figure 5. The system performance with $M = 90$, $N_T = 60$, $N_u = 1, K = 60, L = 4,6,10, \delta = 2$

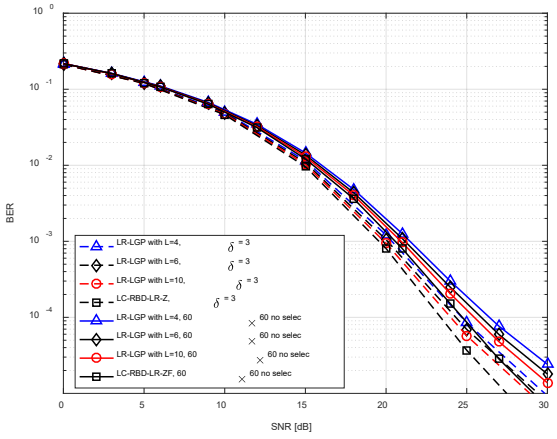

Figure 6. The system performance with $M = 90$, $N_T = 60$, $N_u = 1, K = 60, L = 4,6,10, \delta = 3$

Fig. 7 illustrate the computational complexities of the proposed algorithm LR-LGP and the LC-RBD-LR-ZF algorithm. In this scenario, N_T is varied from 40 to 100 transmit antennas, $N_R = N_T$, $L = 4$ and $L = 10$. It can be seen from the figure that the computational complexities of the proposed precoder is noticeably lower than those of the LC-RBD-LR-ZF precoder. Specifically, at $N_T = 80$ antennas, the computational complexities of the LR-LGP precoder with $L = 4$ and $L = 10$ groups are equal to about 6.25%, 13.54% of the LC-RBD-LR-ZF precoder's complexity, respectively. We can also see from the figure that the computational complexity of the LR-LGP precoder increases as the number of groups L increases.

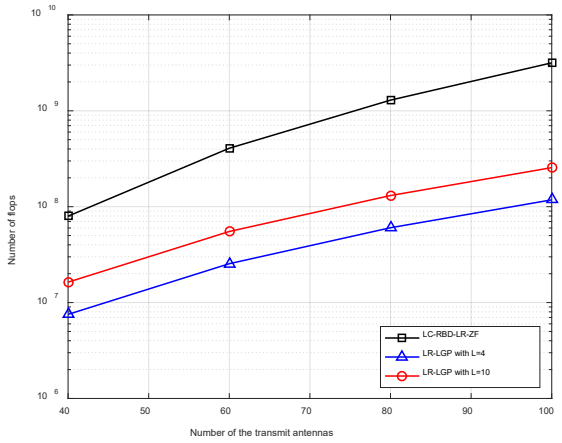

Figure 7. Compare the complexity of the proposed precoding algorithm and the LC-RBD-LR-ZF algorithm in [12]

6. Conclusions

In this paper, we propose the transmit antenna group selection technique for Massive MIMO system. The algorithm is performed on the basis of analyzing the channel capacity. Antenna groups that contribute the most to the total channel capacity will be selected. To trade the computational complexity off against the system performance, from the selected antennas, we develop a low-complexity lattice reduction-aided linear group precoding in Massive MIMO system, called LR-LPG precoder. The proposed precoder is developed based on the conventional linear precoder in combination with the ELR-SLV technique that has low complexity. Numerical and simulation results show that

the system performance significantly improves when applying the transmit selection technique. Simulation results also show that the system performance inversely proportional to δ. Furthermore, the LR-LGP precoder has remarkably lower complexity than the LC-RBD-LR-ZF, whereas its BER performance approaches that of the LC-RBD-LR-ZF precoder when L increases. As a consequence, the LR-LGP can be a potential candidate for signal beamforming at the BS of Massive MIMO systems.

Acknowledgement: This paper has been presented in part at International Conference on Advanced Technologies for Communications, ATC, 2018

References

[1] H. Q. Ngo, *Massive MIMO: Fundamentals and system designs*. Linkoping University Electronic Press, 2015, vol. 1642

[2] Q. H. Spencer, C. B. Peel, A. L. Swindlehurst, and M. Haardt, "An introduction to the multi-user mimo downlink," *IEEE Communications Magazine*, vol. 42, no. 10, pp. 60–67, Oct 2004.

[3] L. Lu, G. Y. Li, A. L. Swindlehurst, A. Ashikhmin, and R. Zhang, "An overview of massive mimo: Benefits and challenges," *IEEE Journal of Selected Topics in Signal Processing*, vol. 8, no. 5, pp. 742–758, Oct 2014

[4] T. L. Marzetta, "Noncooperative cellular wireless with unlimited numbers of base station antennas," *IEEE Transactions on Wireless Communications*, vol. 9, no. 11, pp. 3590–3600, November 2010.

[5] ——, "Massive mimo: An introduction," *Bell Labs Technical Journal*, vol. 20, pp. 11–22, 2015.

[6] H. Y. T. L. Marzetta, E. G. Larsson and H. Q. Ngo, *Fundamentals of Massive MIMO*. Cambridge University Press, 2016.

[7] E. G. Larsson, O. Edfors, F. Tufvesson, and T. L. Marzetta, "Massive mimo for next generation wireless systems," *IEEE Communications Magazine*, vol. 52, no. 2, pp. 186–195, February 2014.

[8] V. P. Selvan, M. S. Iqbal, and H. S. Al-Raweshidy, "Performance analysis of linear precoding schemes for very large multi-user mimo downlink system," *Fourth edition of the International Conference on the Innovative Computing Technology (INTECH 2014)*, pp. 219–224, Aug 2014.

[9] H. Q. Ngo, E. G. Larsson, and T. L. Marzetta, "Massive mu-mimo downlink tdd systems with linear precoding and downlink pilots," pp. 293–298, 2013.

[10] Y. S. Cho, J. Kim, W. Y. Yang, and C. G. Kang, *MIMO-OFDM wireless communications with MATLAB*. John Wiley & Sons, 2010.

[11] M. . Simarro, F. Domene, F. J. Martínez-Zaldívar, and A. Gonzalez, "Block diagonalization aided precoding algorithm for large mu-mimo systems," *2017 13th International Wireless Communications and Mobile Computing Conference (IWCMC)*, pp. 576–581, June 2017.

[12] K. Zu and R. C. d. Lamare, "Low-complexity lattice reductionaided regularized block diagonalization for mu-mimo systems," *IEEE Communications Letters*, vol. 16, no. 6, pp. 925–928, June 2012.

[13] V. K. Dinh, M. Tuan Le, V. D. Ngo, and C. Hieu Ta, "Transmit antenna selection by group combination precoding in massive mimo system," *2018 International Conference on Advanced Technologies for Communications (ATC)*, pp. 276–281, Oct 2018.

[14] W. S. Bing Fang, Zuping Qian and W. Zhong, "Raise: A new fast transmit antenna selection algorithm for massive mimo systems," *Springer Science+Business Media New York*, September 2014.

[15] T. Tai, W. Chung, and T. Lee, "A low complexity antenna selection algorithm for energy efficiency in massive mimo systems," *2015 IEEE International Conference on Data Science and Data Intensive Systems*, pp. 284–289, Dec 2015.

[16] M. T. A. Rana, R. Vesilo, and I. B. Collings, "Antenna selection in massive mimo using non-central principal component analysis," *2016 26th International Telecommunication Networks and Applications Conference (ITNAC)*, pp. 283–288, Dec 2016.

[17] Q. Zhou and X. Ma, "Element-based lattice reduction algorithms for large mimo detection," *IEEE Journal on Selected Areas in Communications*, vol. 31, no. 2, pp. 274–286, February 2013.